SINGLE VERSUS MULTIPLE WINGLETS: NUMERICAL AND EXPERIMENTAL INVESTIGATION

D. P. Coiro, F. Nicolosi, F. Scherillo, U. Maisto
Department of Aerospace Engineering (DIAS), University of Naples "Federico II", 80125, Naples, Italy

Keywords *winglets, multiple winglets, induced drag, Oswald factor*

Abstract

The main goal of the proposed paper is the numerical and experimental investigation of multiple winglets influence on the reduction of induced drag. This results in the improvement of climbing performances of a motorglider or hang-glider. In a precedent work [1] a set of multiple winglets, very similar to the bird tip feathers called remiges, were designed and optimized for the hang-glider belonging to Angelo D'Arrigo, a world champion hang-glider pilot and record holder. The research aims was to optimize the $CL^{1,5}/CD$ parameter since this is directly proportional to the sink rate. In this work the effects of the multiple winglets, set on an elliptical wing and tested in a wind tunnel, are compared to the effects of three different single 'classical' winglets that were designed using a panel method code and were also tested in the same wind tunnel in order to compare their span efficiency to the one of the multiple winglets.

1 Introduction

The main aim of this work was to investigate the effect of multiple winglets applied to an elliptical wing.
The first investigations on a single winglet were performed by Whitcomb[2],[3] in the mid 1970s and it was shown that, if properly designed, the winglet can improve efficiency by reducing the induced drag. Many other researchers have investigated their behavior, designing winglets for commercial and general aviation aircraft as well as for sailplanes [4]. Furthermore, the added friction and interference drag has to be cancelled out by the forward thrust generated by the winglet lift. Since this has been proven to work, it is thus possible to extend this concept to multiple winglets. The principle is to spread the tip vortex in more vortices of less intensity. A variety of types of multiple winglets have been investigated by many authors in the past, such as, Spillman[5],[6], Zimmer[7], La Roche[8], and more recently by Smith[9],[10] and Catalano[11]. The importance of numerical accuracy and the difficulties in predicting the effect of winglets on drag using numerical methods have been well illustrated by Smith[12]. Different concepts, including box and ring wings, have been thoroughly analyzed by Kroo[13].
In this work two different sets of multiple winglets were designed and tested. The main idea was to improve the climb performance and then to maximize the endurance parameter $C_L^{3/2}/C_D$ as showed by (1):

$$V_s = \frac{1}{\frac{C_L^{3/2}}{C_d}} \cdot \sqrt{\frac{2W}{\rho S}} \cdot \left[1 - \left(\frac{2W}{\rho S}\frac{1}{rgC_L}\right)^2\right]^{\frac{3}{4}} \quad (1)$$

where V_s is the sinking rate.
The winglets design process was performed using a classical vortex lattice method [14] to rapidly perform computations for many different configurations. The cant angle and twist of winglets were the main parameters to be optimized during the design phase (Figure 1).
The design was carried out using two sets of winglet; one made of five and the other of three.
The optimization was carried out by replacing part of the wing tip with the winglets in order to keep wingspan the same and to preserve essentially the same aspect ratio of the 'complete wing'. In this way the complete wing

and the wing with its tip substituted by multiple winglets could be compared accurately.

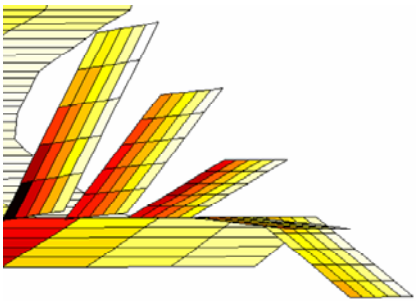

Figure 1

Using the information obtained from the design phase, two sets of five and three winglets were built. An elliptical wing model on which to apply the winglets was also built. The wing model was designed and built so that a part of the wing tip could be extracted and replaced by the set of winglets. In this way it was possible to compare the 'complete wing' with the wing equipped with the sets of winglet at equal span and aspect ratio.

Three different 'classical' winglets were also designed and built in order to have a comparison between multiple winglets and single (classical) winglet. In this case the winglets were designed and optimized using a classical panel method code [15],[16]. These winglets were designed and built to be applied to the same elliptical wing used for the multiple winglets sets, but it is important to mark here that in this case the span and the aspect ratio of the wing equipped with the single winglet was not the same of the 'complete wing' like the case of multiple winglets set.

The various configurations were tested in the wind tunnel of the Department of Aerospace Engineering of the University of Naples Federico II.

2 Experimental setup and models tested

The experimental tests were carried out in the wind tunnel of the Department of Aerospace Engineering of the University of Naples Federico II. The wind tunnel is a closed circuit tunnel with closed test section. The test section has the following dimensions: width 2 m, height 1.4 m with a turbulence level of 0.1% and maximum speed of 45 m/s.

Taking into account the dimensions of the test section an experimental semi-span model of the elliptical wing was designed and built. The model was built at the ELASIS Fiat Research Center of Pomigliano (Naples, Italy) using the rapid prototyping technique which is normally used to quickly fabricate a scale model of a part or an assembly using three-dimensional computer aided design (CAD) data. Rapid Prototyping is a technology directly driven by a CAD model, rapidly manufacturing any complex shaped object.

A 4 cm stand off was interposed between the wind tunnel wall and the model in order to avoid boundary layer wall interference on the model. The stand off was assembled on the wing model so that the aerodynamic loads on the stand off were not transferred to the wing model [17].

The model was built keeping the leading edge straight, and it was possible to replace a part of the wing with the set of multiple winglets (Figure 2).

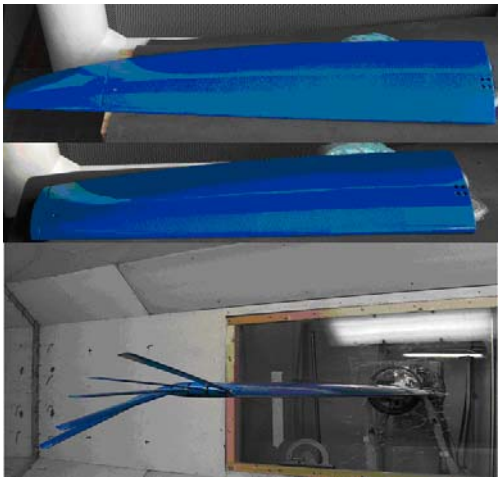

Figure 2: Elliptical wing model: Total (Elliptical), Short wing and short wing + 5 winglets.

The wing airfoil used is the NFL 1015. This airfoil shows maximum endurance at low C_L and a $C_{L\alpha}$=0.1/deg.

The geometrical characteristics of the complete Elliptical wing (also called "Total wing") and of the Short Wing (SW) are reported in Table 1. The symbol b and the wing area S represent

respectively the model span (or wing semi-span) and the model area (or wing semi-area).
The sets of winglets and the wing tip were also built using the rapid prototyping technique. The multiple winglets were built using the indications obtained from the numerical analysis [1].

Table 1 geometrical characteristics

	b (m)	S (m^2)	Cr (m)	Ct (m)	AR
Elliptical (Total wing)	1.51	0.452	0.37	0.097	10.1
Short wing	1.23	0.40	0.37	0.233	7.6

The numerical results suggested that it is better to increase the cant angle as much as possible, in order to maximize the distance between the winglets. In the following tables (Table 2**,** Table 3) the other geometrical characteristics of the winglets are summarized.

Table 2 ***5 multiple winglets set***

N. of Winglet	*Surface (m^2)*	*Span (m)*	*Twist (°)*	Taper ratio	*Root chord (m)*
1° winglet	0.01	0.25	8.5	1	0.04
2° winglet	0.01	0.25	8.5	1	0.04
3° winglet	0.01	0.25	8.5	1	0.04
4° winglet	0.01	0.25	7.5	1	0.04
5° winglet	0.01	0.25	5.5	1	0.04

Table 3 ***3 multiple winglets set***

N. of Winglet	*Surface (m^2)*	*Span (m)*	*Twist(°)*	Taper ratio	*Root chord (m)*
1° winglet	0.015	0.25	8.5	0.53	0.07
2° winglet	0.015	0.25	6.5	0.53	0.07
3° winglet	0.015	0.25	5.5	0.53	0.07

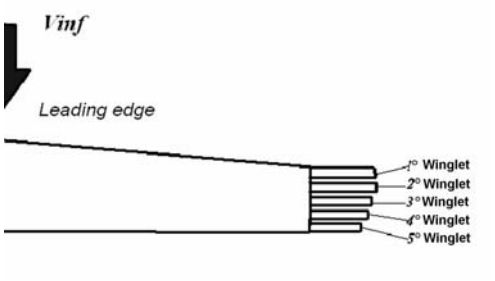

Figure 3: winglets numbering

In order to install the winglets, a special wing tip was designed which allowed cant and pitching angle of the winglets to be changed.
In the first phase of the experimental work a preliminary investigation was carried out in order to optimize winglet pitch and cant angle in the various winglets configurations. The results of this optimization are summarized in the Table 4 and Table 5 and are reported in [1].

Table 4 Optimization results

Short wing + 5 winglets		
N. of Winglet	*Pitch*	*Cant angle*
1° winglet	-4.2°	13.7°
2° winglet	-2.8°	3.04°
3° winglet	-5.6°	-1.63°
4° winglet	-4.6°	-15.9°
5° winglet	-2.6°	-23.9°

Table 5 Optimization results

Short wing + 3 winglets		
N. of Winglet	*Pitch*	*Cant angle*
1° winglet	-5.4°	43°
2° winglet	-4.9°	10°
3° winglet	-1.6°	-20.6°

The junction gap between the winglets root and the wing tip then was filled with a molded clay in order to avoid an excessive reduction of the aerodynamic performance in terms of drag due to the junction interference, and it was noticed a significant influence of this fairing on the global performance. In order to have an experimental comparison with a classical winglet configuration different 'single' winglets were designed and built. The winglets were designed, using the indications obtained from the panel method analysis, with different sweep, twist and toe angles, see Figure 4 for definitions, as shown in Figure 5 and listed in Table 6. The comparison between the different toe and twist angles of the three different tested winglets along the span curvilinear abscissa is shown in Figure 6. Further, the different chordwise position and sweep angles are shown in Figure 7 and Figure 8.
In this case the aspect ratio was not the same of the elliptical wing(AR=10.08), like in the previous case, but was slightly higher of the short wing(8.2 compared to 7.6 relative to the short wing) (Figure 5, Table 6).

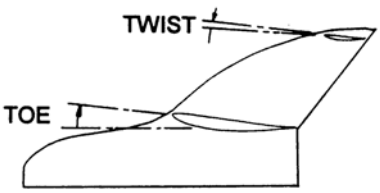

Figure 4: Twist and toe angle definition

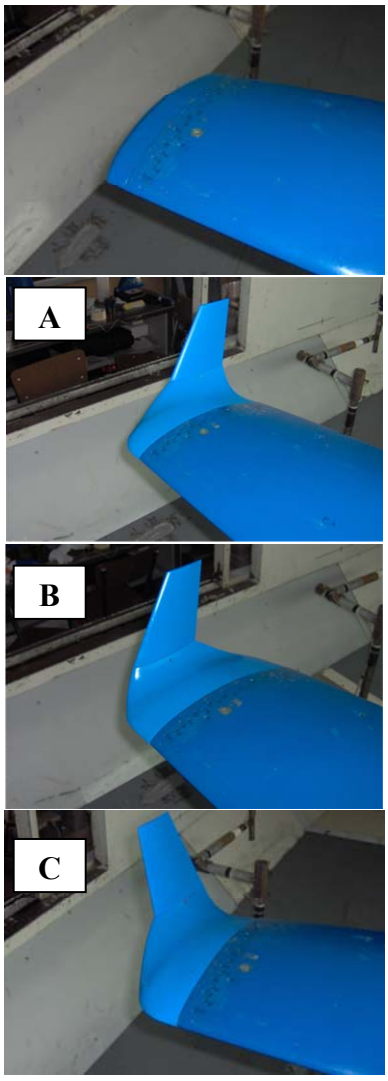

Figure 5: Short wing and short wing + single winglets

Table 6 Single winglet configuration

Type of configuration	*Surface (m^2)*	*Span (m)*	*AR*	*Twist Angle (°)*	*Toe angle (°)*
Elliptical Wing	0.45	1.51	10.1	-	-
Short Wing (SW)	0.40	1.23	7.6	-	-
SW + winglet A	0.41	1.30	8.23	3	-8
SW + winglet B	0.41	1.31	8.28	3	-1
SW + winglet C	0.41	1.30	8.23	3	-8

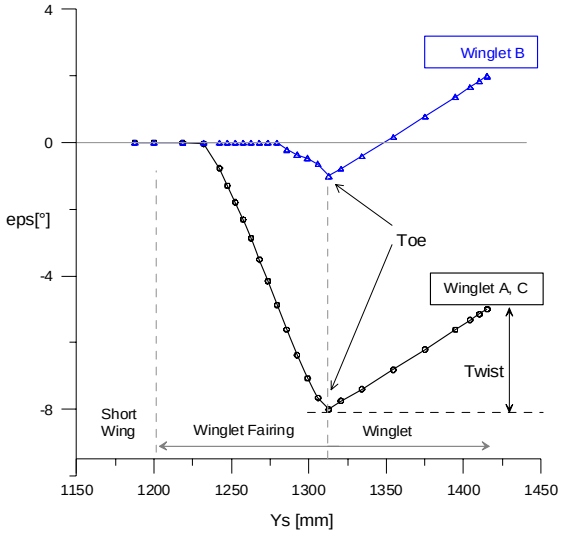

Figure 6: Winglets twist and toe angles

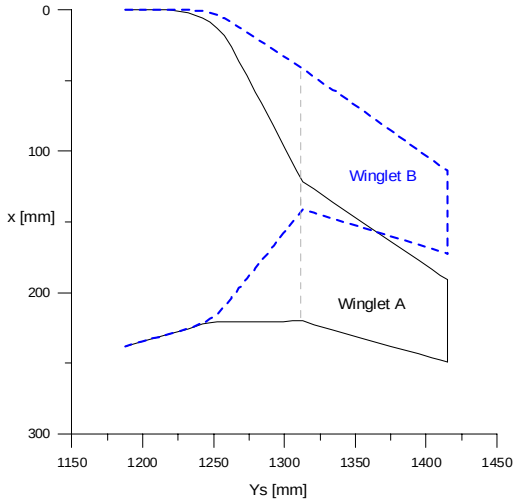

Figure 7: Winglets chordwise position

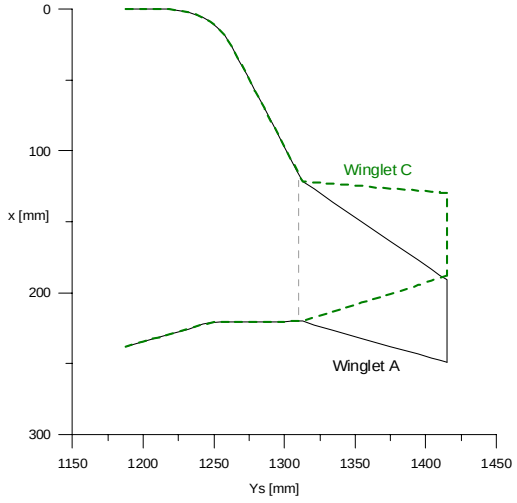

Figure 8: Winglets Sweep

The elliptical wing was also equipped with 122 pressure holes in order to check the span load distribution.
The pressure holes were distributed over 17 wing sections. It was not possible to distribute a sufficient number of pressure holes over all of the sections as this would have required more tubes than it was physically possible to fit inside the wing. For this reason it was chosen to distribute 36 pressure holes on three wing sections placed at 25%, 50% and 80% of the wing, and the others on the wing upper surface on the remaining sections.
The pressures were measured using two different pressure transducer systems each equipped with 64 ports and made by Scanivalve Corp with a full scale of ~2550 Pa and a accuracy of 0.15% FS.
Aerodynamic forces and moments were measured in the tests. In order to measure these forces, a four-component strain gages balance (previously designed by the authors) (Figure 9) outside the wind tunnel was used.

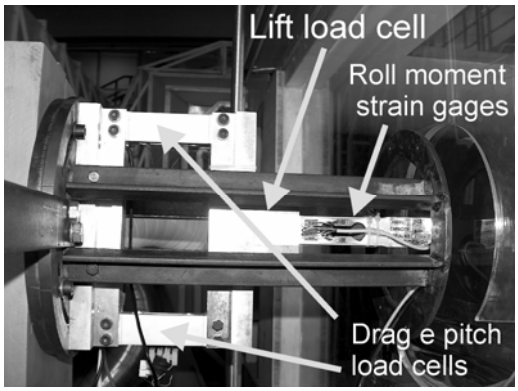

Figure 9: Four components strain gages balance.

The lift load cell has a maximum load capacity of about 2000 N and a sensitivity of 2.0mV/V±10%; drag and pitch load cells both have a maximum load capacity of 300 N and a sensitivity of 2.0mV/V±5%. The load cell is also capable of measuring the roll moment.

3 Multiple winglets: Discussion of results

A first series of tests were carried out on the elliptical wing without winglets to check the elliptical span load. The curves C_L vs α and C_L vs C_D are reported in Figure 10 and Figure 11

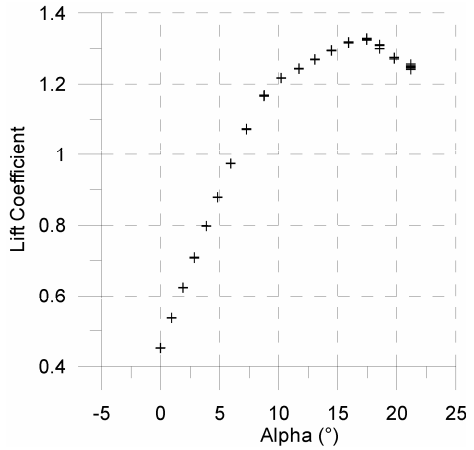

Figure 10: Elliptical wing: C_L vs α curve.

The shape of the curve C_L vs α reflects the shape of the airfoil curve NFL 1015 showing a change in the curve slope before the stall angle. As expected, the wing α_{oL} is equal to the airfoil α_{ol}~-6°.
Computing the slope of C_L vs α using the experimental data curve in the linear range gives $C_{L\alpha}$ =0.087/deg . From elliptical wing theory the result is:

$$C_{L\alpha} = \frac{C_{l\alpha}}{1 + C_{l\alpha}/(\pi \cdot AR)} = 0.085 / deg \,.$$

The comparison between the theoretical and the experimental $C_{L\alpha}$ is therefore fairly satisfactory.
The Oswald factor computed from the experimental data comes out as e=0.94. This was considered reasonable supposing that the difference between the theoretical (e=1) and the experimental results could be due to the Oswald factor being calculated by considering viscous drag constant with α while in reality it is not.

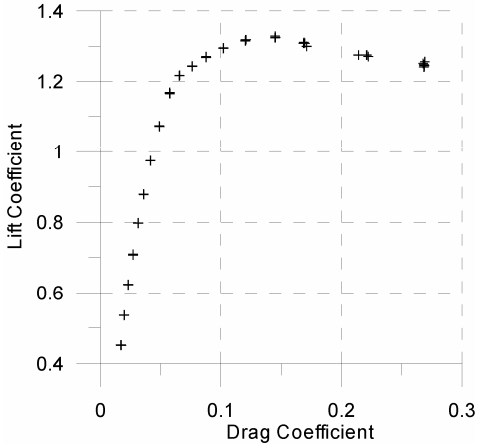

Figure 11: Elliptical wing: C_L vs C_D curve.

Using the pressure test results it is possible to compute the local span load cC_l in the section at 25%, 50% and 80% of the span. The comparison between the experimental and the theoretical span load (elliptical wing theory) is once again satisfactory, see Figure 12.
Once the total wing had been fully characterized, the experimental tests on the configurations with the multiple winglets were carried out.

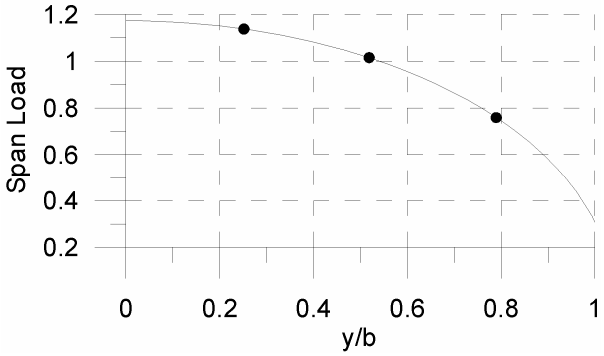

Figure 12: Comparison between theoretical and experimental span load: α=3°.

The configuration with three winglets did not show any improvement over the total wing while that with five winglets showed an improvement for values of C_L>0.65 (Figure 13, Figure 14).

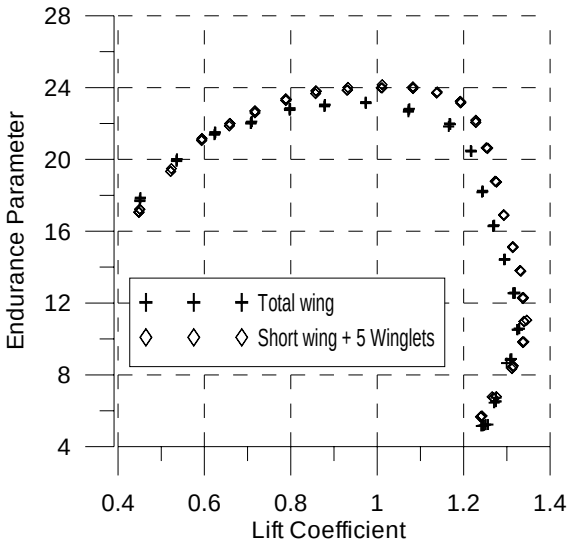

Figure 13: Curve $C_L^{3/2}/C_D$ vs C_L. Comparison between elliptical wing configuration and 5winglets configuration.

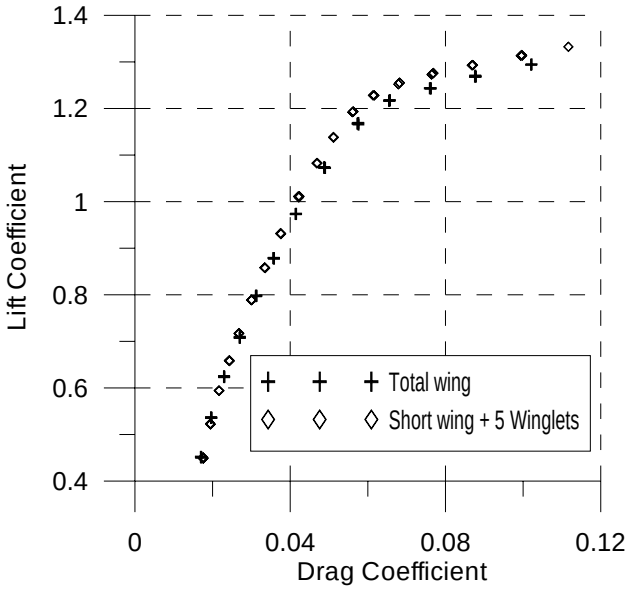

Figure 14: Curve C_L vs C_D. Comparison between elliptical wing configuration and 5winglets configuration.

The Table 7 and Table 8 summarize the main results obtained from the comparison between the different configurations.

Table 7 Oswald factor

Configurations	*AR*	*e*
Total wing	10.04	0.94
Short wing + 5 winglets	9.96	1.04
Short wing + 3 winglets	10.03	0.83

Table 8 Comparison with elliptical wing

	Fixed C_L	*% Advantage*		
	C_L	C_D	C_L/C_D	$C_L^{3/2}/C_D$
Short wing + 5 winglets	1.2	-8%	+10%	+9 %

4 Multiple winglets: wake survey

A wake survey was performed in order to investigate the wake vortex structure downstream of the wing.
This investigation was carried out using a five-hole probe. The probe was positioned about two and half chord downstream of the wing trailing edge and placed on a two axes moving system controlled by a dedicated PC (Figure 15).

Figure 15: Elliptical wing: Wake survey.

For every point of measurement the probe supplied the three velocity components (u,v,w) while the spatial position (x,y,z) was supplied by the movement control system. In this way it was possible to scan the velocity field in a plane downstream of the wing orthogonal to freestream velocity.

The investigation was carried out for both the elliptical wing configuration and for the 5 winglets wing configuration, both at an angle of attack of 6°. The points of measurement were distributed on a structured grid on the scanning plane.

The first measurement was carried out on a 1,200 point grid. The measurement time for this grid took about one and half hours. The grid measurement external sizes were: 1,200 mm width, 600 mm height with a spacing of 30 mm. The use of these grid dimensions to scan the wake plane made it possible to identify the vortex structures downstream of the elliptical wing configuration and downstream of the 5 winglets wing configuration (Figure 16, Figure 17).

Once the position of the vortices had been identified then a more accurate wake scan was carried out on the 5 winglets wing configuration in the zones where vortices were present. The grid dimensions used in this case were: 600mm in width and 600 mm in height with a grid spacing of 10 mm (3,600 points) (Figure 18).

As Figure 18 shows, the 5 winglets configuration shows the wing tip vortex to be split into five vortices, which, as expected, have a lower intensity of vorticity compared with the elliptical wing vortex. It should be noted that the vorticity value indicated in Figure 19 is the mean value of vorticity for each grid cell.

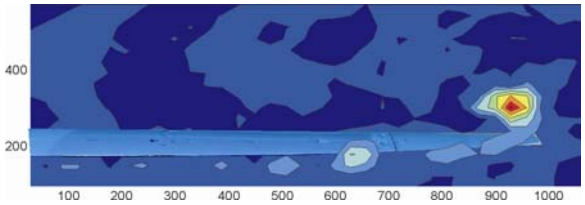

Figure 16: Elliptical wing: Vorticity.

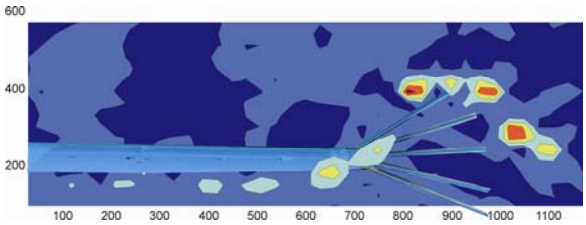

Figure 17: 5-Winglets configuration : Vorticity (1200 mm x 600 mm).

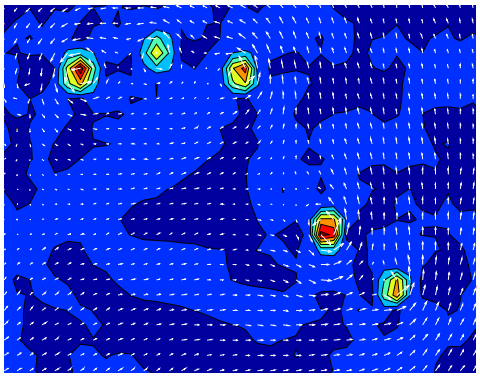

Figure 18: 5-winglets configuration : Vorticity and velocity vectors (600 mm x 600 mm).

In order to obtain a qualitative estimate of the induced drag for the two different configurations the Maskell formula [17] was applied to the scanned planes.

$$D_i = \frac{1}{2}\rho \iint_W \psi \cdot \zeta \, dydz$$

Where ψ comes from the solution of the Poisson equation: $\nabla^2 \psi = -\xi$.

A comparison of the results from Maskell analysis, reported in the Table 9, show an induced drag reduction of 13% for the 5 winglets configuration.

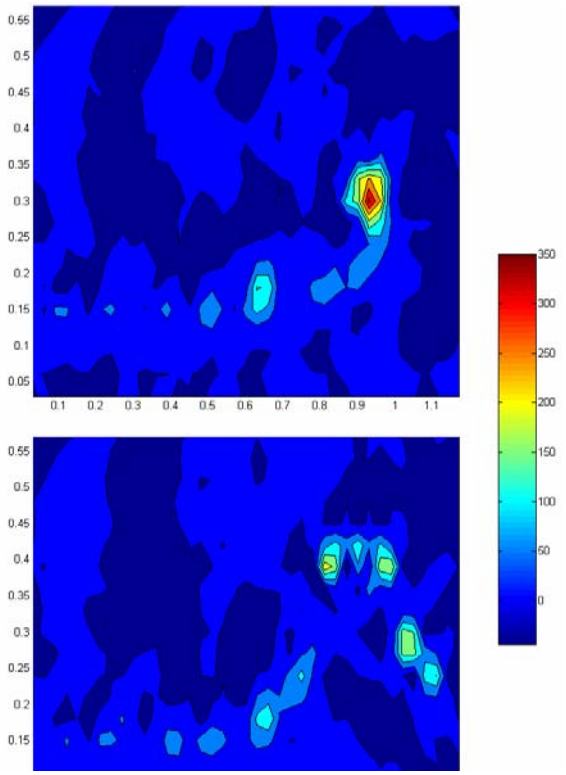

Figure 19: Comparison between elliptical wing and five winglets: vorticity intensity.

Table 9

Configuration	C_{Di}
Elliptical wing	0.0168
5 Winglets	0.0146

5 Single winglets: Discussion of results

The results of tests performed on the three single 'classical' winglet configurations are reported in the following figures.

All the three configurations with the winglets show an improvement respect to the short wing in terms of induced drag and CL_α (Figure 20, Figure 21, Figure 22). Obviously part of this improvement is due to the higher aspect ratio of the winglet configurations respect to the short wing aspect ratio, but from Figure 20 it is possible to observe that the CL_α of the winglet configuration is about the same of the elliptical wing CL_α, that has an higher aspect ratio respect to the other configurations.

Fig. 21 clearly shows that the winglet leads to an improvement of the Oswald factor. Table 10 shows that adding the winglet allows to obtain an Oswald factor (which means and induced drag factor) about 15% higher. Fig. 21 and 22 show the drag polar of the elliptical wing compared to that one of the short wing and short wing + winglet. The lift and drag coefficients for each configuration are referred to the area of that configuration. The three different winglets show very similar influence and similar obtained induced drag reduction.

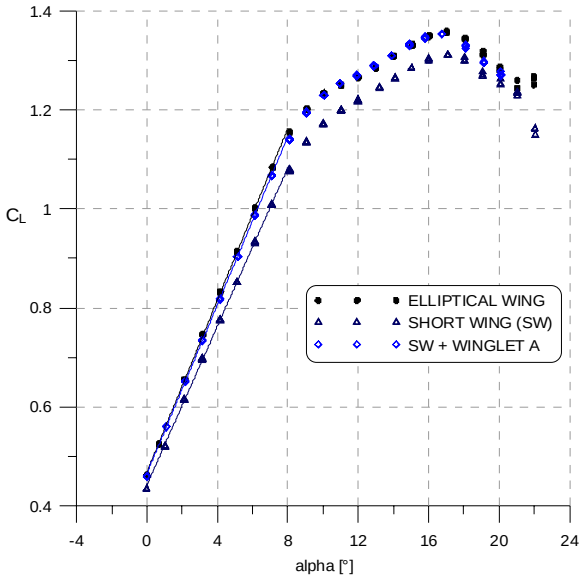

Figure 20: C_L vs α

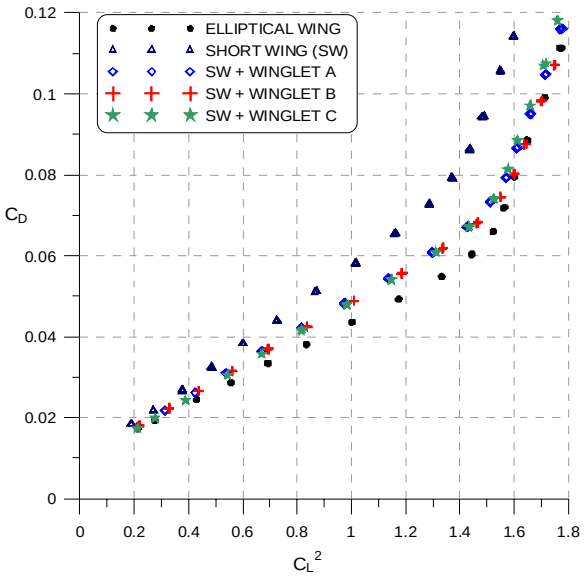

Figure 21: C_L^2 vs C_D

Results shown in fig. 20, 21 and 22 are numerically summarized in table 10. All the winglets lead to improved tip vorticity and lower induced drag. The similar behavior of the 3 winglets confirms the numerical calculations (used to design the three tested winglets) that

were indicating different toe angles for different winglet positions.

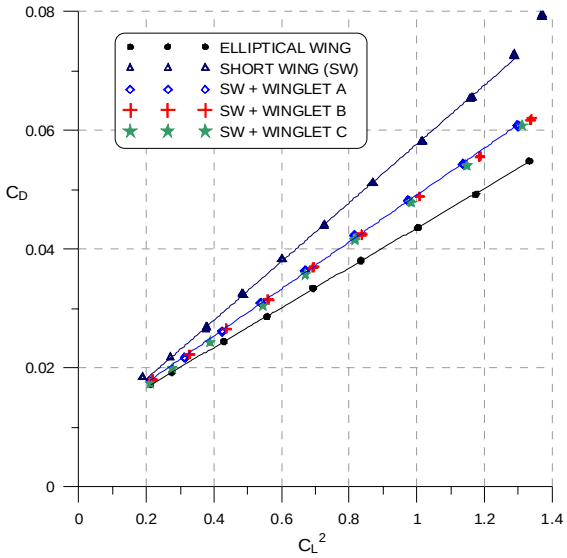

Figure 22: C_L^2 vs C_D: linear zone

Table 10 Oswald factor

Type of configuration	$C_{L\alpha}$	*e*
Elliptical wing	0.0867	0.94
Short wing (SW)	0.0801	0.85
SW + winglet A	0.0851	0.98
SW + winglet B	0.0851	0.99
SW + winglet C	0.0851	0.99

To obtain more significant comparable results in terms of increase of wing root bending moment of the analyzed configurations (with very different aspect ratios) the bending moment non-dimensional coefficient C_{Mf} and the lift coefficient have been obtained using the same span and the same reference area (short wing area, 0.40 m^2).

The bending moment coefficient is defined as:

$$C_{Mf} = \frac{M_f}{q \cdot S \cdot b}$$

During the tests the bending moment at wing root has been measured by a dedicated load cell. The bending moment with the winglets is obviously higher respect to the short wing bending moment as shown in Figure 23. This increase is partly due to the higher span of the winglets configuration and partly to the presence of the winglet (vertical part). At C_L=1.0, the bending moment with the winglet is 6% higher than that one relative to the short wing. The obtained induced drag gain, as shown before, is sensibly higher.

The ratio of bending moment coefficient versus lift coefficient represents the point (in % of wing semi-span) of application of the global lift. This length is of course useful to obtain aerodynamic bending moment for a certain aerodynamic flight load (i.e. the aerodynamic load in the maneuver diagram).

The slopes of the curves shown in figure 23 are thereafter representative of the wing global aerodynamic center span position. The slopes indicate that this point is at 52% of the semi-span for the short wing, 54% for the short wing + winglet and 59% for the elliptical wing (that has much higher aspect ratio). This obtained results indicate that the elliptical wing leads to an increase of bending moment of about 14% respect to the short wing. The winglet lead to a much lower effect (only 6% higher) on the bending moment with a significant above mentioned effect on the induced drag reduction.

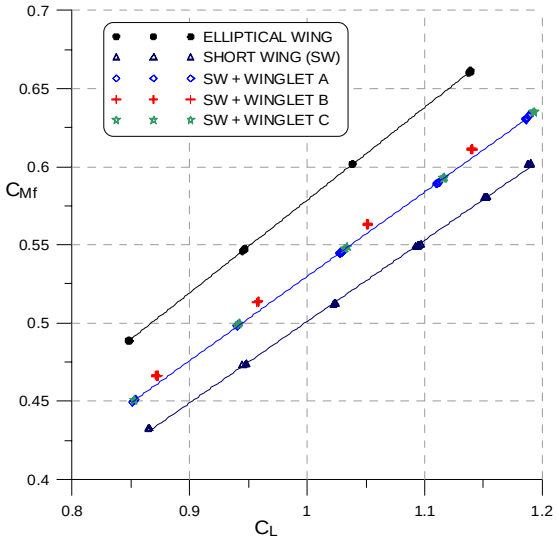

Figure 23: Bending moment coefficient C_{Mf} vs C_L

The endurance parameter ($C_L^{3/2}/C_D$) for the elliptical wing, the short wing and the short wing+winglet have been evaluated. The used lift and drag coefficients were again referred to the same wing area (short wing =0.40 m^2). The endurance parameter versus lift coefficient is plotted in Figure 24.

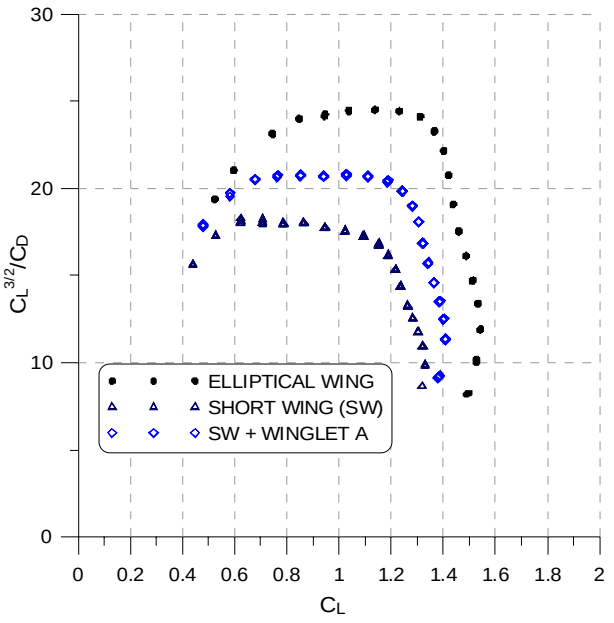

Figure 24 :Endurance parameter versus lift coefficient. Data referred to the same reference area.

It can be observed that the winglet leads to an increase of the endurance parameter from 17.5 (relative to the short wing) to about 21 (SW+wingletA). This gain is about 20%. The endurance parameter(obtained with the same reference area for all the configurations) represents also a measure of the "flight soaring performances" of such configurations.
The small increase of aspect ratio for the short wing +winglet (8.2 compared to 7.6 relative to the short wing) is only 8%. The above mentioned obtained gain, has to be attributed to the winglet influence. All the results show the strong capabilities of 'classical' winglets to reduce induced drag and to improve soaring performances with contained bending moment increase. In fact similar gain (i.e. for the short wing characteristics) can be obtained increasing the global wing span, but with much higher increase of the wing bending moment at the wing root.

6 Comparison between multiple and single winglets

Due to the different aspect ratio of the two configurations, short wing plus 5 winglets and the short wing plus winglet A, a comparison can be made only in terms of Oswald factor. In Table 11 are reported the maximum percentage advantage for every configuration respect to the reference wing (short wing for the single winglets, elliptical wing for the multiple winglets).

Table 11 Percentage advantage in terms of Oswald factor

Type of configuration	*e % advantage*
Short wing + 5 winglets	~10 %
Short wing + winglet A	~13 %

From the results shown in Table 11 the classical winglet configuration seems to be more advantageous respect to the multiple winglets. It is important to remark here that a further significant improvement for the 5 winglets configuration performance is possible reducing the junction interference drag filling and better shaping the gaps between the winglets root and the wing tip.

7 Conclusion

In this work numerical and experimental investigation were performed on an elliptical wing equipped with both single and multiple winglets. Both winglets type were designed using numerical codes.
The experimental results obtained from wind tunnel test were compared in terms of Oswald factor. From this comparison seems that the single winglet is more advantageous respect to the multiple winglets, although the latter were not optimized in terms of parasite drag due to the interference of the junction between the multiple winglets and the main wing. The induced drag reduction of all tip device should always carefully analyzed in terms of possible increase of bending moment at wing root. In the paper this aspect has been highlighted for the 'classical' winglet configuration.

References

[1] D. P. Coiro, F. Nicolosi, F. Scherillo, U. Maisto "Improving Hang-Glider Maneuverability Using Multiple Winglets:A Numerical and Experimental Investigation", Journal of Aircraft Vol. 45, n. 3 May-June 2008, pp. 981-989.

[2] Whitcomb R. "A Design Approach and Selected Wind-Tunnel Results at High Subsonic Speeds for Wing-Tip Mounted Winglets," NASA TN D-8260 July 1976

[3] Whitcomb R. "Method for Reducing Aerodynamic Drag," NASA CP 2211 *Dryden Symposyum* Sept. 1981

[4] K. W. Mortara, M.D. Maughmer "A method for the prediction of induced drag for planar and nonplanar wings," AIAA Paper 1993 3420-CP

[5] J. J. Spillman "The use of Wing Tip to reduce vortex drag," *Aeronautical Journal Paper* No. 618, 1978, pp. 387-395.

[6] J. J. Spillman, H.Y. Ratcliffe, A. McVitie "Flight experiments to evaluate the effect of wing-tip sails on fuel consumption and handling characteristics, " *Aeronautical Journal Paper* No. 694, 1979, pp. 279-281.

[7] H.Zimmer "The Aerodynamic Optimization of Wings at Subsonic Speeds and the Influence of Wingtip Design," *NASA Technical Memorandum*, NASA TM-88534, 1987

[8] U. La Roche, H.L. La Roche "Induced Drag using Multiple Winglets, looking beyond the Prandtl-Munk Model," AIAA Paper 2004 -.2120

[9] M.J. Smith, N. Komerath, R. Ames, O. Wong, J. Pearson "Performance Analysis of a Wing with Multiple Winglets," AIAA Paper 2001-2407

[10] A. Shelton, A. Tomar, JVR Prasad, M. Smith N. Komerath "Active Multiple for Improved Unmanned-Aerial-Vehicle Performance," *Journal of Aircraft,* Vol. 43, No. 1, 2006, pp. 110,116.

[11] F.M. Catalano, H.D. Ceron-Munoz "Experimental Analysis of Aerodynamics Characteristics of Adaptive Multi-Winglets," *43rd AIAA Aerospace Sciences Meeting and Exhibit* AIAA 2005-1231 Reno,Nevada 2005

[12] S.C. Smith " A computational and Experimental Study of Nonlinear Aspects of Induced Drag," *NASA Technical Paper* 3598, 1996

[13] I.Kroo, " Drag Due to Lift: Concepts for Prediction and Reduction," *Annual Reviews of Fluid Mechanics* 2001 Vol. 33 p.p. 587-617.

[14] Katz and Plotkin, "Low Speed Aerodynamics, From Wing Theory To Panel Methods," *McGraw-Hill Inc., 1991*

[15] Maughmer M.D., Kunz P.J., "Sailplane Winglet Design Process", Presented at the XXV OSTIV Congress, Saint Auban, France.

[16] Maughmer M.D., "*Design of Winglets for High-Performance Sailplanes*", Journal of Aircraft, Vol. 40, No. 6, November-December 2003, pp 1099-1106.

[17] G.M. Gatlin, R.J Mcghee, "Study of Semi-Span Model Testing," *AIAA 14th Applied Aerodynamics Conference* AIAA 96-2386 New Orleans LA 1196

Copyright Statement

The authors confirm that they, and/or their company or institution, hold copyright on all of the original material included in their paper. They also confirm they have obtained permission, from the copyright holder of any third party material included in their paper, to publish it as part of their paper. The authors grant full permission for the publication and distribution of their paper as part of the ICAS2008 proceedings or as individual off-prints from the proceedings.